

PARSING INFLAMMATORY CUES IN ANGIOGENESIS USING BIOACTIVE HYDROGELS

By

Angela Zachman

Thesis

Submitted to the Faculty of the
Graduate School of Vanderbilt University
in partial fulfillment of degree requirements
for the degree of

MASTER OF SCIENCE

in

Biomedical Engineering

May, 2011

Nashville, Tennessee

Approved:

Dr. Hak-Joon Sung

Dr. Scott Guelcher

ACKNOWLEDGEMENTS

This work would not have been possible without the help of my PI, Dr. Hak-Joon Sung and my fellow lab mates, Spencer Crowder, Lucas Hofmiester, Dae Kwang Jung, and Mukesh Gupta. Katarzyna Zienkiewicz and Dr. Scott Guelcher were also of great help on this project as well as other collaborations, particularly for the HPLC analysis in this study. They provided great insight, suggestions, and support for my research. Ophir Ortiz and the New Jersey Center for Biomaterials at Rutgers University kindly supplied polymer samples and analyzed the mechanical properties of these polymers. I would like to thank the two undergraduate students who worked with me on this project, Christine Bronikowski and Aidan Boone. I would also like to thank Jason Tucker-Swartz and Dr. Melissa Skala for their help with OCT imaging. This work also would not have been possible without the Vanderbilt Institute of Nanoscale Science and Engineering (VINSE) for SEM imaging, and the Vanderbilt University School of Medicine (VUMC) Cell Imaging Shared Resource for confocal imaging. This work was supported by NIH HL091465 and NSF 1006558. I could not have accomplished this work without the love and support of my parents and family.

TABLE OF CONTENTS

	Page
ACKNOWLEDGEMENTS	ii
LIST OF TABLES.....	v
LIST OF FIGURES	vi
Chapter	
I. INTRODUCTION	1
Host response to biomaterials	1
Biomaterial design and fabrication.....	1
Bioactive synthetic peptides	2
II. PARSING INFLAMMATORY CUES IN ANGIOGENESIS USING BIOACTIVE HYDROGELS	4
Introduction	4
Methods	4
Fabrication and characterization of hydrogels.....	4
Mechanical testing of hydrogel scaffolds	5
Degradation of hydrogel scaffolds	5
Protein adsorption on hydrogel scaffolds.....	6
Peptide release from ECM gel filled hydrogel scaffolds	6
Cell culture and collagen-hydrogel format for in vitro cell assays.....	6
<i>In vitro</i> angiogenic and inflammatory activities from culture of single cell types in peptide and collagen-filled hydrogel scaffolds.....	7
Co-culture of human monocytes and HUVECs on collagen-hydrogel scaffolds	8
<i>In vivo</i> angiogenesis and inflammatory activation in implanted collagen-hydrogel scaffolds.....	8
Statistical analysis	9
Results	9
Fabrication of porous hydrogel scaffolds	9
Mechanical testing of hydrogel scaffolds	10

Peptide Release from ECM gel filled hydrogels	12
In vitro testing of pro-angiogenic effect on EC migration and tubulogenesis	13
<i>In vitro</i> testing of anti-inflammatory effect on macrophage activation	14
Co-culture of macrophages and HUVECs on collagen-hydrogel scaffolds	15
<i>In vivo</i> subcutaneous implantation of collagen-hydrogel scaffolds	18
Discussion.....	20
III. CONCLUSION.....	23
REFERENCES	24

LIST OF TABLES

Table	Page
1. Sequence and Function of Synthetic Peptides.....	2

LIST OF FIGURES

Figure	Page
1. Characterization of hydrogel scaffolds.....	9
2. Mechanical properties, degradation, and protein adsorption of hydrogel scaffolds.....	11
3. Peptide release from collagen or fibrin-filled porous hydrogel scaffolds.....	12
4. <i>In vitro</i> responses of HUVECs and macrophages to peptide- loaded collagen-hydrogel scaffolds.....	14
5. <i>In vitro</i> co-culture of macrophages and HUVECs with combinations of peptides in collagen-hydrogel scaffolds.....	16
6. <i>In vivo</i> angiogenesis and inflammatory cell activation with peptides in collagen-hydrogel scaffolds.....	1

CHAPTER I

INTRODUCTION

Host response to biomaterials

Biomedical implants that facilitate communication and interaction with the surrounding tissue and circulatory system are rendered ineffective by the huge diffusion barrier and increased electrical resistance presented by the fibrous capsule [1, 2]. For successful implants, it is ideal to have the device surrounded and penetrated by highly vascularized tissue [3]. Angiogenesis occurs naturally in reproduction, wound repair, placental development, and the foreign body response to form new blood vessels from activated vascular endothelial cells (ECs). When grown on a biomaterial, ECs migrate, associate, and elongate into tubule structures that resemble immature budding capillaries during angiogenesis [4]. Both angiogenesis and inflammation are inescapable *in vivo* responses to all biomaterial implants, and there is emerging evidence that inflammatory cells regulate the functions of endothelial cells related to angiogenesis [5, 6]. Although these processes are thought to be related in fields such as cell biology, cancer, cardiovascular medicine, immunology, and pathophysiology, the interconnectivity of these two processes is not understood well in the field of biomaterials research [5-10].

Biomaterial design and fabrication

One key aspect of biomaterial applications for clinical implants is that the surface, internal, micro, and macro properties of biomaterials should be biomimetic to be compatible with the natural extracellular environment. On the other hand, modification of even one biomaterial parameter can affect cellular behavior and the subsequent physiological outcome. For example, increased roughness of biomaterial surfaces enhances the adhesion and growth of ECs [11, 12], suggesting the possibility of controlling angiogenesis via modification of biomaterial surface parameters. Hydrogels are often thought to be relatively tissue-compatible, most likely due to their properties resembling living tissue, such as high water content and elasticity [13, 14]. Studies have also shown that implants with increased water content inhibit the adhesion of macrophages, and therefore, may affect the inflammatory response [15]. A unique type of

polyethylene glycol (PEG)-cross-linked tyrosine-derived polycarbonate hydrogels have been synthesized and characterized. These polymeric hydrogels have controllable crosslink and degradation properties and can be easily fabricated into porous scaffolds, because studies have shown that a porous structure is also important to controlling inflammatory responses and vascularization [16, 17]. Tyrosine-derived polycarbonates are tissue-compatible, exhibit desirable mechanical properties, and are hydrophobic with a slow degradation rate [18]. Chemically cross-linking with PEG produces hydrolytically degradable hydrogels to facilitate cell interactions and accelerate wound healing [13, 19].

Bioactive synthetic peptides

Hydrogel scaffolds can be made more bioactive by introducing synthetic peptides that are derived from extracellular matrix (ECM) components. Studies have shown that peptides from laminin-1 (an ECM protein composed of three chains -- α 1, β 1, and γ 1) can promote angiogenesis *in vivo* [20, 21]. One of the most potent sites from laminin-1 is peptide C16 from the γ 1 chain (Table 1). This peptide promotes EC adhesion, tube formation, and angiogenesis. The C16Y peptide was made through one amino acid substitution in the C16 sequence (Table 1) and showed strong inhibition of angiogenesis *in vivo* [20]. On the other hand, a tetrapeptide, Ac-SDKP (Table 1), has been identified as an anti-inflammatory cytokine, decreasing macrophage infiltration and TGF- β expression [22-25]. This peptide is normally present in organs and biological fluids.

Table 1. Sequence and Function of Synthetic Peptides

Peptide	Activity	Sequence
C16	Pro-angiogenic	Lysine-Alanine-Phenylalanine-Aspartic acid-Isoleucine-Threonine-Tyrosine-Valine-Arginine-Leucine-Lysine-Phenylalanine.
C16Y	Anti-angiogenic	Aspartic acid-Phenylalanine-Lysine-Leucine- Phenylalanine -Alanine-Valine-Tyrosine-Isoleucine-Lysine-Tyrosine-Arginine
C16L	Scrambled, control peptide for C16 and C16Y, inactive	Leucine-Threonine-Phenylalanine-Arginine-Alanine-Lysine-Valine-Tyrosine-Phenylalanine-Isoleucine-Lysine-Aspartic acid
Ac-SDKP	Anti-inflammatory	N-acetyl-serine-Aspartic acid-lysine-proline
Ac-DKSP	Scrambled control peptide for Ac-SDKP, inactive	N-acetyl-Aspartic acid-lysine-serine-proline

CHAPTER II

PARSING INFLAMMATORY CUES IN ANGIOGENESIS USING BIOACTIVE HYDROGELS

Introduction

To investigate the role of biomaterial-induced inflammation in angiogenesis and the related mechanisms, it is important to investigate how the interaction of inflammatory cells with the biomaterial affects endothelial cell responses. The goal of this study is to address the hypothesis that the inflammatory response to biomaterials may regulate angiogenic activities in biomaterial implants. To investigate this hypothesis, polyethylene glycol (PEG)-cross-linked tyrosine-derived polycarbonates were used to fabricate porous hydrogel scaffolds. The porous structure, mechanical properties, degradation profile, and protein adsorption of these hydrogel scaffolds were characterized through a series of tests. Peptides, including C16 (pro-angiogenic), C16Y (anti-angiogenic), Ac-SDKP (anti-angiogenic) and their scrambled controls were hybridized with ECM gels to the hydrogel scaffolds to control angiogenic and inflammatory processes. The release of peptides from the ECM gel-filled hydrogel scaffolds was measured using high performance liquid chromatography (HPLC). These peptide filled ECM-gel hydrogels were also used for *in vitro* biological studies with ECs and macrophages individually and in co-culture, as well as for *in vivo* studies to investigate the interplay between inflammation and angiogenesis.

Methods

Fabrication and characterization of hydrogels

-Polymers and cross-linking: A series of copolymers of X mole % desaminotyrosyl tyrosine ethyl ester (DTE) and Y mole % desaminotyrosyl-tyrosine (DT) ($X+Y = 100\%$), were identified as poly(x%DTE-co-y%DT carbonate) (Figure 1A) [26]. For a given value of Y (%), the extent of cross-linking can be changed by reacting 0 to 100% of the free carboxylic acids with amine groups of polyethylene glycol dihydrazides (PEG dihydrazides; $M_w = 2,000$).

-Fabrication and imaging of porous structure: Macro-and micro-pores were generated following the previously reported procedures [26]. Briefly, macro-pores were generated through salt leaching. Micro-pores were created by evaporation of phase-separated organic solvent domains through lyophilization. The pore structure and interconnectivity were characterized by imaging with scanning electron microscopy (SEM) and optical coherence tomography (OCT).

-Peptide loading through hybridization of ECM gel: Functional and control molecules, i.e. pro-angiogenic C16, anti-angiogenic C16Y, anti-inflammatory Ac-SDKP, pro-inflammatory lipopolysaccharide (LPS), and various scrambled peptide controls (Table 1) were incorporated into the hydrogel scaffolds by hybridization, i.e. filling the pores with a solution of a gel-forming ECM component (either collagen or fibrin) that contains the peptides [20-23, 27]. All peptides were obtained from GenScript (Piscataway, NJ). To evaluate the stability of the hydrogel-ECM gel association, hydrogels were embedded in collagen solution (3.1 mg/ml; Chemicon, Rosemont, Illinois) and imaged before and at 7 days post collagen gel formation with a variable geometry Skyscan 1172 Microtomograph (Micro-CT) unit with a 10W X-ray source (Micro Photonics Inc., Allentown, PA). The X-ray source was set to 45kV for optimal imaging of polymer scaffold-collagen constructs.

Mechanical testing of hydrogel scaffolds

For mechanical testing, hydrogel scaffolds were hybridized with collagen and tested in compression on an Instron Model 5D Materials Testing Machine (Norwood, MA). The specimens were compressed at a crosshead speed of 0.5mm/min and the stress vs. strain curve was recorded. The Young's modulus was calculated as the slope of the linear portion of the stress-strain curve (n=3).

Degradation of hydrogel scaffolds

Hydrogel scaffold degradation was profiled by HPLC over time after incubating hydrogel scaffolds in phosphate buffer saline (PBS) at 37°C [28]. The PBS supernatant was treated with 1N NaOH to hydrolyze the polymer fragments to DT. The amount of DT was measured by HPLC (Waters Corporation, Milford, MA), and the concentration of was determined from a standard calibration curve. Samples were collected at days 0, 3, 7, 21, and 28 (n=3).

Protein adsorption on hydrogel scaffolds

Gold quartz crystals (Q-Sense, Q-Sense, Sweden) were spin-coated with a mixture (1% weight/volume) of poly(90%DTE-co-10%DT carbonate) and PEG-dihydrazide (0, 8 or 20%) as described previously [29]. PBS was run through each chamber until an equilibrium baseline was established. Fibrinogen (0.3 g/ml) in PBS was then run at a flow rate of 24.2 $\mu\text{L}/\text{min}$ for 2 hours. A PBS rinse was performed for 1 hour to remove any reversibly adsorbed proteins. The Voigt model in Q-Tools (Q-Sense) was used to model overtones 3-9 to obtain the adsorbed mass ($\mu\text{g}/\text{cm}^2$) (n=3) using the previously described methods.[30, 31]

Peptide release from ECM gel filled hydrogel scaffolds

Hydrogel scaffolds hybridized with a mixture of peptides and collagen or fibrin (75 μg of peptide/hydrogel, n=4) were incubated in PBS at 37°C for 3, 7, or 14 days. As all peptides in the “C16 family” (C16, C16Y, and C16L) are composed of the same number (12 amino acids) and composition of amino acids with different sequences, these are referred to as “long peptides.” All the peptides in the “Ac-SDKP family” are four amino acids long, but in different sequences, so these are referred to as “short peptides.” The name, sequence, and source of these peptides are found in Table 1. The supernatant was collected at the end of the time point and the released peptides were detected by HPLC using a Xterra® RP18 column (Waters) with a flow rate of 1 $\mu\text{L}/\text{min}$ at 37°C at 220nm detection wavelength. A gradient was created starting with 100% mobile phase A (0.1% TFA in water) for 2 minutes and gradually changing to 95% mobile phase B (90% methanol with 0.1% TFA in water) at 15 minutes. This composition is held for one minute then increased to 100% mobile phase B after an additional minute. The amount of released peptides was calculated based on a standard curve made from unknown concentrations of peptides ranging from 0 to 75 $\mu\text{g}/\text{mL}$ using Breeze™ software (Waters).

Cell culture and collagen-hydrogel format for *in vitro* cell assays

Human umbilical vein ECs (HUVECs) were obtained from Cambrex (East Rutherford, NJ) and cultured in a standard EC growth medium [32]. Human blood-derived monocytes (HBMs) were obtained from Advanced Biotechnologies (Columbia, MD), and seeded at a density of 2×10^7 cells/10mL of DMEM

(Invitrogen, Carlsbad, CA) with 20% fetal calf serum (Intergen, Purchase, NY), 10% human serum (Nabi, Boca Raton, FL), and 5µg/mL macrophage colony-stimulating factor (Sigma Aldrich, St. Louis, MO) for 9 days to differentiate into macrophages [33]. For all *in vitro* cell assays, the collagen gel samples were prepared, some with and some without the embedding of peptides (see section 2.1). The gel-peptide complex was hybridized with porous hydrogel scaffolds made from poly (DTE-co-10%DT carbonate) with 8% PEG crosslinker.

In vitro angiogenic and inflammatory activities from culture of single cell types in peptide and collagen-filled hydrogel scaffolds

-*HUVEC migration*: HUVECs (2×10^4 / scaffold) were labeled with Hoechst 33258 nuclear stain (Sigma) and seeded onto the top surface of collagen-hydrogel scaffolds with or without C16 (75µg). Three-dimensional HUVEC migration from gel surface into the scaffold pores was imaged at 0 and 72 hour(s) post seeding using optical sectioning (3µm intervals) with a Leica TCS SP2 multi-photon microscope system (Wetzlar, Germany). The number of cells that migrated into scaffolds was calculated as a ratio to non-migrating cell population on the surface (n=5). Proliferating cells were visualized by BrdU staining, according supplier's protocol (Chemicon).

- *Tubulogenesis*: HUVECs (2.5×10^5 / scaffold) were cultured for 72 hours on collagen-hydrogel scaffolds with C16 peptides (0, 25, 50, or 75µg). The range of the peptide concentration was determined following the previous study [27]. The nuclei were stained with ethidium bromide (red, Invitrogen, Carlsbad, CA) and the actin cytoskeleton was visualized by FITC-phalloidin (green, Invitrogen). The cells were imaged with a multi-photon confocal microscope and tube length measured using Microsuite software (AnalySIS, Olympus, Germany) (n=5) [26].

- *Phagocytosis*: Macrophages (1×10^5 / scaffold) were cultured for 24 hours on collagen-hydrogel scaffolds with lipopolysaccharide (LPS; 100ng) as a positive control or Ac-SDKP peptides (0, 25, 50, or 75µg). The cells were treated with green-fluorescent *Escherichia coli* (*E. coli*) particles for 2 hours according to manufacturer protocol using Vybrant® Phagocytosis assay kit (Invitrogen), counter – stained with Hoechst, and imaged with a multi-photon confocal microscope (Leica TCS SP2) [34, 35]. The green

fluorescence intensity was measured and normalized to the corresponding cell number using Image J (NIH) (n=5).

Co-culture of human monocytes and HUVECs on collagen-hydrogel scaffolds

Macrophages (2×10^5 /scaffold) were mixed with collagen solution, cell culture media, and peptides (75 μ g for C16, C16L, Ac-SDKP, and Ac-DKSP peptides) or LPS (1 μ g) and this complex was hybridized to a hydrogel scaffold by incubating for 2-3 hours to allow gelation. HUVECs (2×10^5 /scaffold) (Cell Applications, San Diego, CA) were seeded on top of the collagen-hydrogel scaffolds in a 50:50 mixture of macrophage and endothelial cell media. After three days, macrophages were analyzed for phagocytic activity using Vybrant® Phagocytosis assay kit. Samples were fixed and HUVECs were stained for vascular cell adhesion molecule-1 (VCAM-1) using APC conjugated anti-human CD106 antibody (BioLegend, San Diego, CA). Cells were counted by Hoechst nuclear stain. Hydrogels were imaged using Olympus FV 1000 inverted confocal microscope (Center Valley, PA) and images were analyzed for the number of tube formations, average green fluorescence intensity (phagocytosis), and the number of VCAM-1-positive cells per 300 μ m x 300 μ m imaged area (n=8).

In vivo angiogenesis and inflammatory activation in implanted collagen-hydrogel scaffolds

Collagen-hydrogel scaffolds containing LPS (100ng) or functional peptides (0 or 75 μ g) were sandwiched between two nitrocellulose filters (Millipore, Billerica, MA) to constrain nonspecific tissue growth within the scaffolds to two dimensions [9]. The scaffolds were then implanted subcutaneously in the dorsal regions of mice (129 SvEv) for 7 days. After sacrificing the mice, their vasculature was perfused with 10mL heparinized saline containing 0.1 μ m fluorospheres by injection into the left ventricle [10, 36]. Scaffolds were harvested and vasculature was visualized with multi-photon microscopy and quantified by dissolving the microspheres in xylene and measuring the fluorescence intensity using a plate reader (Tecan, Durham, NC) [10, 36]. At the same time, the phagocytosis activity was measured using Vybrant® Phagocytosis assay kit (see the section 2.7). The expression of F4/80 membrane-bound antigens on inflammatory cells infiltrated into implants was detected by immunohistochemistry of frozen sections from the harvested scaffolds using Alexa Fluor 594-conjugated rat anti-mouse F4/80 monoclonal

antibodies (Abcam, Cambridge, MA). The fluorescence intensity was measured and normalized to the corresponding total cell number, measured by Hoechst (n=6) [9].

Statistical analysis

In all experiments, analytical results were expressed as means \pm standard error. Comparisons of individual sample groups were performed using unpaired student's t-test. For all statistics, $p < 0.05$ was considered statistically significant.

Results

Fabrication of porous hydrogel scaffolds

Hydrogels were successfully fabricated with varying DT content (0 and 10%) and PEG dihydrazide cross-linker composition (0, 8, 20, and 40%). We characterized this new hydrogel system for pore structure, collagen gel stability, modulus, degradation profile, and protein adsorption. SEM and OCT revealed a highly porous, interconnected structure with controllable macro-pores between 212 and 425 μ m formed by salt leeching (Figure 1b and c). To ensure that the collagen gel maintained stability over time, micro-CT of a collagen-gel filled hydrogel scaffold at 7 days post hybridization (right) was compared to an unfilled hydrogel scaffold (left) (Figure 1d). The pores (white area), which were observed dominantly on the surface before embedding, were stably filled with collagen gel (black area) at 7 days post-embedding.

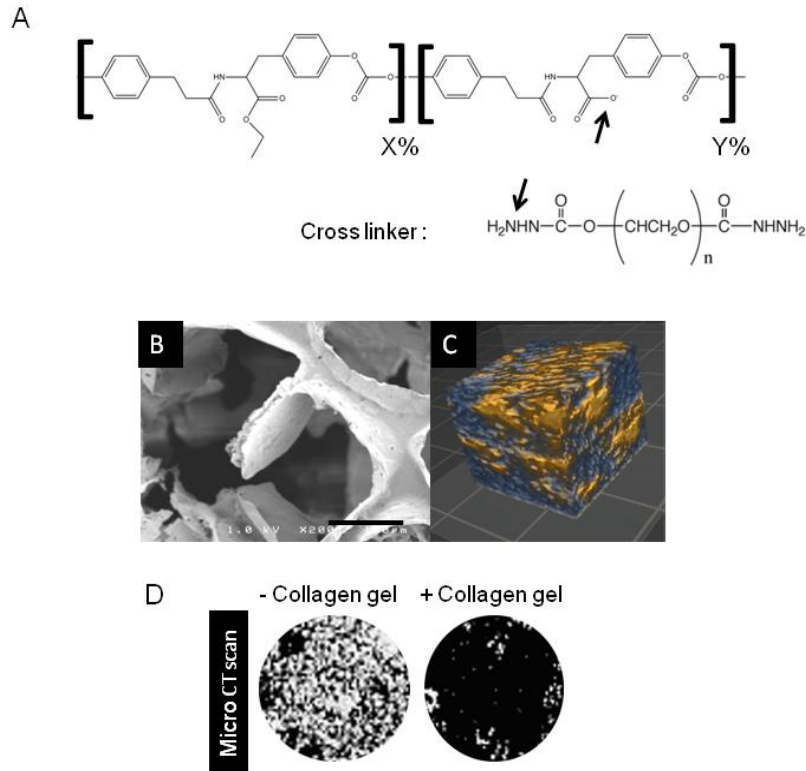


Figure 1. Characterization of hydrogel scaffolds. **A.** Chemical structure of poly (X%DTE-Y%DT carbonate) with polyethylene glycol (PEG)-dihydrazide cross-linker. The free carboxyl group (arrow) of DT forms an amide bond with the amine group (arrow) of PEG-dihydrazide for cross-linking polymer chains. X and Y indicate molar percentages of DTE and DT, respectively, with 0-100% variation in each unit ($X+Y=100\%$). The cross-linking degree with PEG-dihydrazides can vary from 0 to 100% for available Y%DT. **B.** SEM image showing surface view of the pore architecture in a hydrogel scaffold. Scale bar= $150\mu\text{m}$. **C.** OCT image showing the 3D interconnectivity of pores in a hydrogel scaffold (2mmx2mm scan). Blue=pores, yellow=scaffold. **D.** Micro CT scan images showing the whole surface of the hydrogel (diameter = 0.6 cm) without (left) and with (right) collagen gel at 7 days post hybridization of collagen gel. White area = pores; black area = collagen gel or polymers.

Mechanical testing of hydrogel scaffolds

For mechanical tests, hydrogel scaffolds with 0, 8, 20, and 40% PEG cross-linker were compressed and the slope of the stress versus strain curve was measured (Young's modulus, Figure 2a). The inclusion of the PEG cross-linker in an 8% molar ratio increased the modulus of the hydrogel scaffolds, as compared to hydrogel scaffolds with 0% PEG dihydrazide. However, the modulus decreased significantly as the cross-linking degree further increased from 8% to 20% and to 40%. Hydrogels with 40% cross-linking had a Young's modulus that was not statistically different from those with 0% cross-linking. The degradation rate of hydrogel scaffolds, as indicated by the cumulative release of DT (a major degradation product) was dependent on the degree of cross-linking (Figure 2b). There was no significant

difference in the amount of released DT among the hydrogel scaffold types tested until 20 days incubation in PBS. After 28 days, the largest amount of DT was released from non-crosslinked hydrogel scaffolds, indicating faster degradation of 0% crosslinked hydrogel scaffolds than other scaffold types with higher cross-linking degrees. The 40% cross-linked hydrogels released the least amount of DT from 20 to 28 days, confirming a role of cross-linking in slowing the degradation rate of hydrogel scaffold.

To investigate the interplay between PEG and negatively-charged DT in modulating protein adsorption on polymer surfaces, fibrin adsorption to the polymer surface was measured using QCM-D (Figure 2a). As the PEG molar ratio increased from 0 % to 8% and to 20% in mixture with poly(90%DTE-co-10%DT carbonate), fibrin adsorption significantly decreased, confirming a repellent effect of PEG on fibrin adsorption [29]. On the other hand, copolymerization of 10% DT significantly increased fibrin adsorption, compared to pure poly (DTE carbonate), indicating a potential effect of negatively charged carboxyl groups on increased protein adsorption.

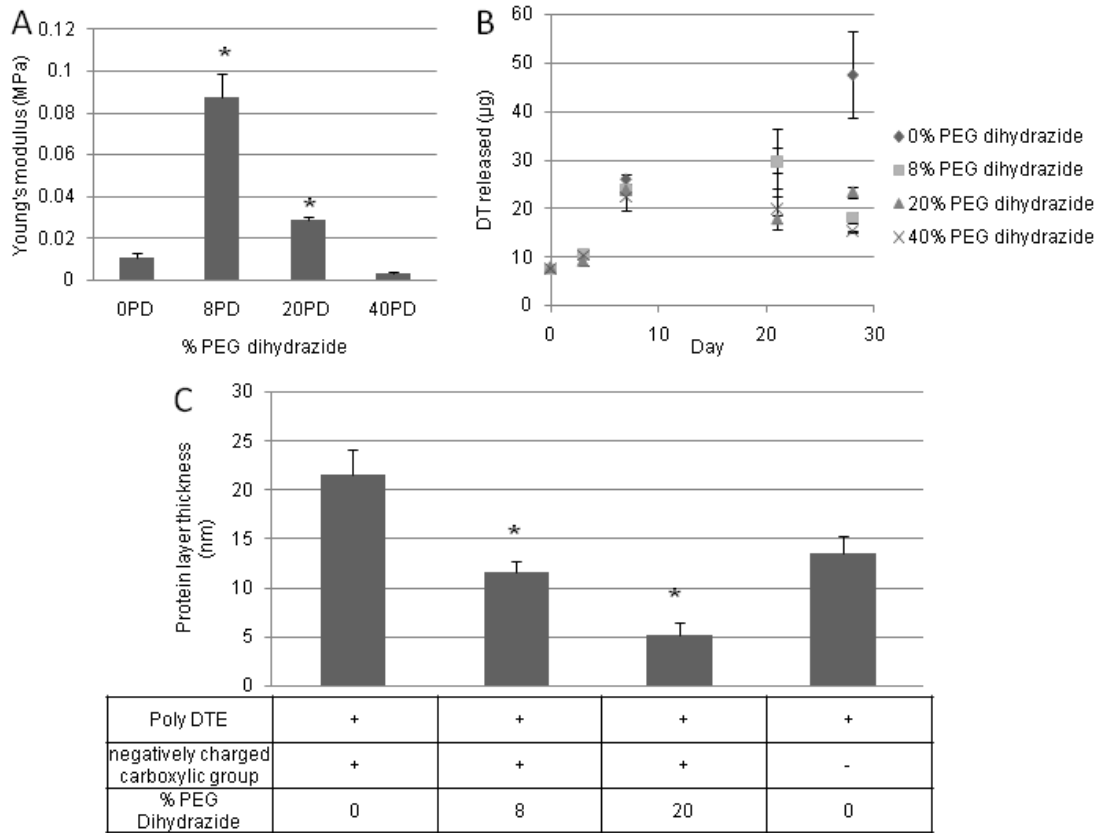


Figure 2. Mechanical properties, degradation, and protein adsorption of hydrogel scaffolds. **A.** Young's modulus obtained from compression testing of collagen-filled hydrogel scaffolds. Hydrogel scaffolds with 0, 8, 20, or 40% cross-linking with PEG dihydrazides were compressed at a constant rate. The Young's modulus was calculated (MPa) from the slope of stress versus strain curve (n=3). **B.** Degradation profiles of hydrogel scaffolds. Hydrogel scaffolds were incubated in PBS at 37°C and supernatant was collected for analysis by HPLC (n=3). **C.** Protein adsorption on polymers with increasing percentages of PEG dihydrazide. A mixture of polymer and PEG-dihydrazide was spin-coated on a quartz crystal, incubated with fibrinogen in PBS at 37°C, and the thickness of adsorbed protein layer on each polymer sample was measured through QCM-D (n=3). **a-c)** *p<0.05 vs. all other groups in the same graph.

Peptide Release from ECM gel filled hydrogels

Cumulative release of the peptides from the ECM gel-hydrogel scaffold was measured by HPLC (Figure 3). Hydrogel scaffolds were filled with collagen or fibrin gels containing 75µg of peptide and incubated in PBS. The supernatant was collected and the amount of released peptides was measured over time by HPLC. C16L and Ac-DKSP peptides were used as the representative peptides of the long peptides (C16 family with 12 amino acids) and the short peptides (acetylated tetrapeptide family), respectively. Peptides were released from hydrogel scaffolds in a burst, with an initial high release following a logarithmic pattern, followed by a slower lag phase. This pattern is typical of most drug

release. The long peptides showed a higher initial release, but after 14 days both peptides released almost the same amount. Both types of peptides showed more release from collagen-filled hydrogel scaffolds than fibrin-filled hydrogel scaffolds, therefore collagen-filled hydrogel scaffolds were used in all further *in vitro* and *in vivo* tests.

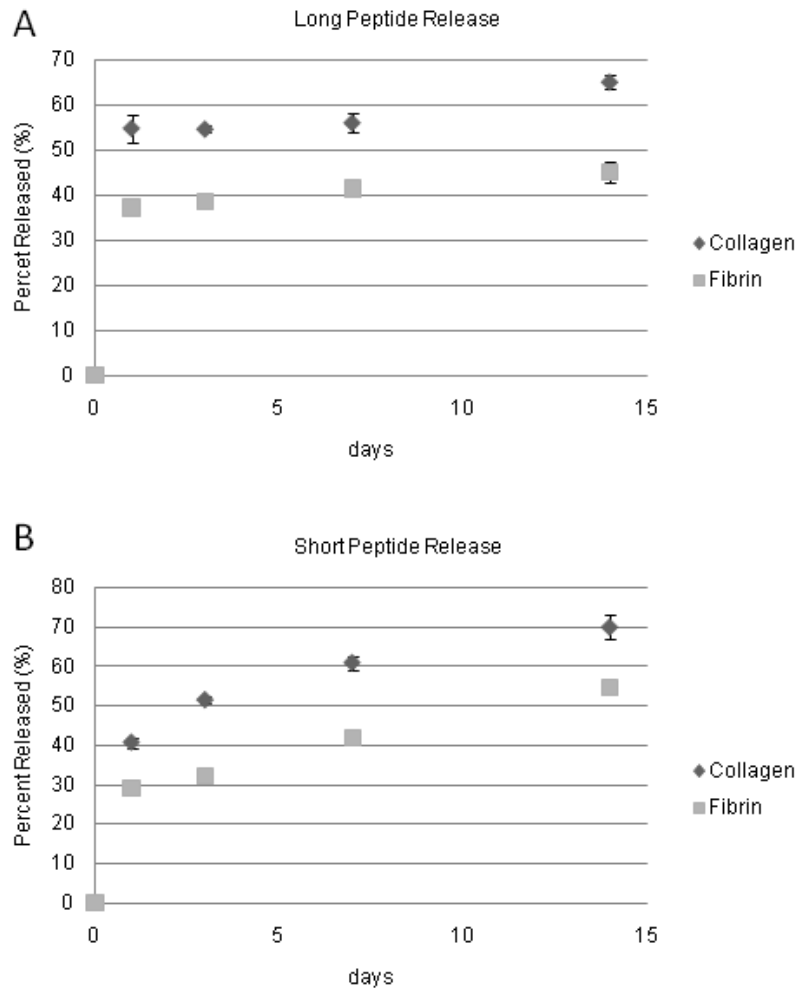


Figure 3. Peptide release from collagen or fibrin-filled porous hydrogel scaffolds. Cumulative release of **a.** the representative type (C16L) of long peptide types and **b.** the representative type (Ac-DKSP) of short peptides. Peptide release from collagen or fibrin filled scaffolds at days 1, 3, 7, and 14 post incubation in PBS was measured using HPLC (n=4).

In vitro testing of pro-angiogenic effect on EC migration and tubulogenesis

A significant number of HUVECs migrated from the surface into the collagen-hydrogel scaffolds for 72 hours after seeding (Figure 4a). The hybridization of pro-angiogenic C16 enhanced the HUVEC

migration into internal layers of collagen-hydrogel scaffolds. The confocal images and corresponding graph in Figure 4b show more cells around 80 μ m into the collagen-hydrogel scaffold with the C16 peptide (75 μ g) than without this peptide. To further investigate the pro-angiogenic effect of the C16 peptides, HUVECs seeded in collagen-hydrogel scaffolds with C16 peptides were incubated for 72 hours and analyzed for the total length of tubes formed by HUVECs. The total tube length increased significantly in a step-wise pattern as the peptide concentration increased from 0 to 75 μ g (Figure 4c). The maximum tubulogenic activity was observed at the highest peptide concentration (75 μ g).

In vitro testing of anti-inflammatory effect on macrophage activation

Monocytes were differentiated into macrophages for *in vitro* testing because macrophages are adherent cells while monocytes are non-adherent. Phagocytic activity was visualized as green fluorescence and quantified by normalizing to corresponding cell number. The green-fluorescence intensity increased upon treatment with LPS (Figure 4d, left picture), and dramatically decreased upon the introduction of anti-inflammatory Ac-SDKP (75 μ g) (Figure 4d, right picture). Phagocytosis activity decreased significantly in a step-wise pattern as the peptide concentration increased from 0 to 75 μ g. The minimum phagocytosis activity was seen at the highest concentration of Ac-SDKP (75 μ g).

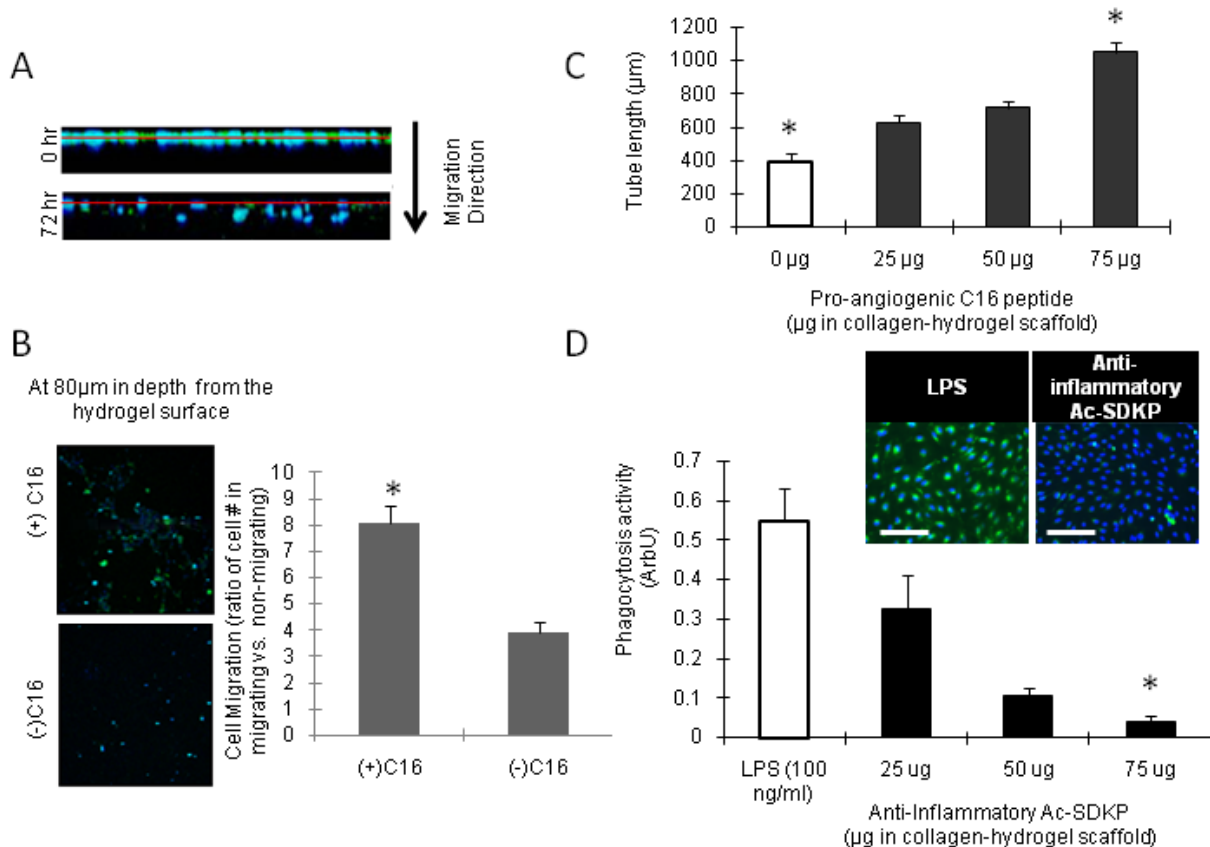


Figure 4. *In vitro* responses of HUVECs and macrophages to peptide-loaded collagen-hydrogel scaffolds. A and B. HUVEC migration into scaffolds. Cell nuclei were stained with Hoechst (blue) and proliferating cells were identified by BrdU staining (green). **A.** Z-sectional projection of HUVEC migration from the surface (red line). **B.** Effect of C16 peptide on HUVEC migration at 72 hours. **C.** Tube length (µm) with different doses of pro-angiogenic C16 peptides. **D.** Phagocytosis of macrophages. The top fluorescence images show macrophages (blue nucleus) phagocytizing *E. coli* particles (green) under treatment of LPS (100ng) without (left) or with (right) anti-inflammatory Ac-SDKP (75ug). The phagocytosis activity (green fluorescence intensity normalized to cell number, bottom graph) under treatment with LPS (100ng) or different doses of Ac-SDKP peptides **c)- d)** n=5. Scale bar = 100µm. **b-d)** *p< 0.05 vs. all the other groups in the same graph.

Co-culture of macrophages and HUVECs on collagen-hydrogel scaffolds

HUVECs were seeded on top of collagen-hydrogel scaffolds. Macrophages were included inside the collagen gel for co-culture. Phagocytosis activity (Figure 5a, left), tubulogenesis (Figure 5a, right), and endothelial cell activation (Figure 5e) were quantified through image analysis. Tubulogenesis was defined as any three or more VCAM-1 (a marker of activated endothelial cells) expressing cells joined together to form a tube [37]. The two activities, tubulogenesis and phagocytosis, showed very similar trends in response to the various combinations of peptides. The combination of Ac-SDKP with C16 decreased phagocytosis as well as tubulogenesis compared to C16 alone. Similarly, the combination of C16Y with LPS decreased tubulogenesis as well as phagocytosis compared to LPS alone. The addition of LPS to

C16 increased both phagocytosis and tubulogenesis compared to C16 alone, and the addition of Ac-SDKP to C16Y decreased both phagocytosis and tubulogenesis compared to C16Y alone. These results indicate an interconnection and a potential feedback mechanism between macrophages and HUVECS in response to biomaterial implants.

VCAM-1 expression has been implicated in EC activation and recruitment of inflammatory cells [32]. The expression of VCAM -1 in HUVECs significantly decreased when anti-inflammatory Ac-SDKP peptides were present in addition to pro-angiogenic C16 peptides, compared to C16 alone (Figure 5d). The number of cells expressing VCAM-1 also decreased in the presence of both C16Y and LPS compared to LPS alone. These results also indicate an interconnected relationship between angiogenesis and inflammation, as well as a potential causative role of macrophages in EC tubulogenesis.

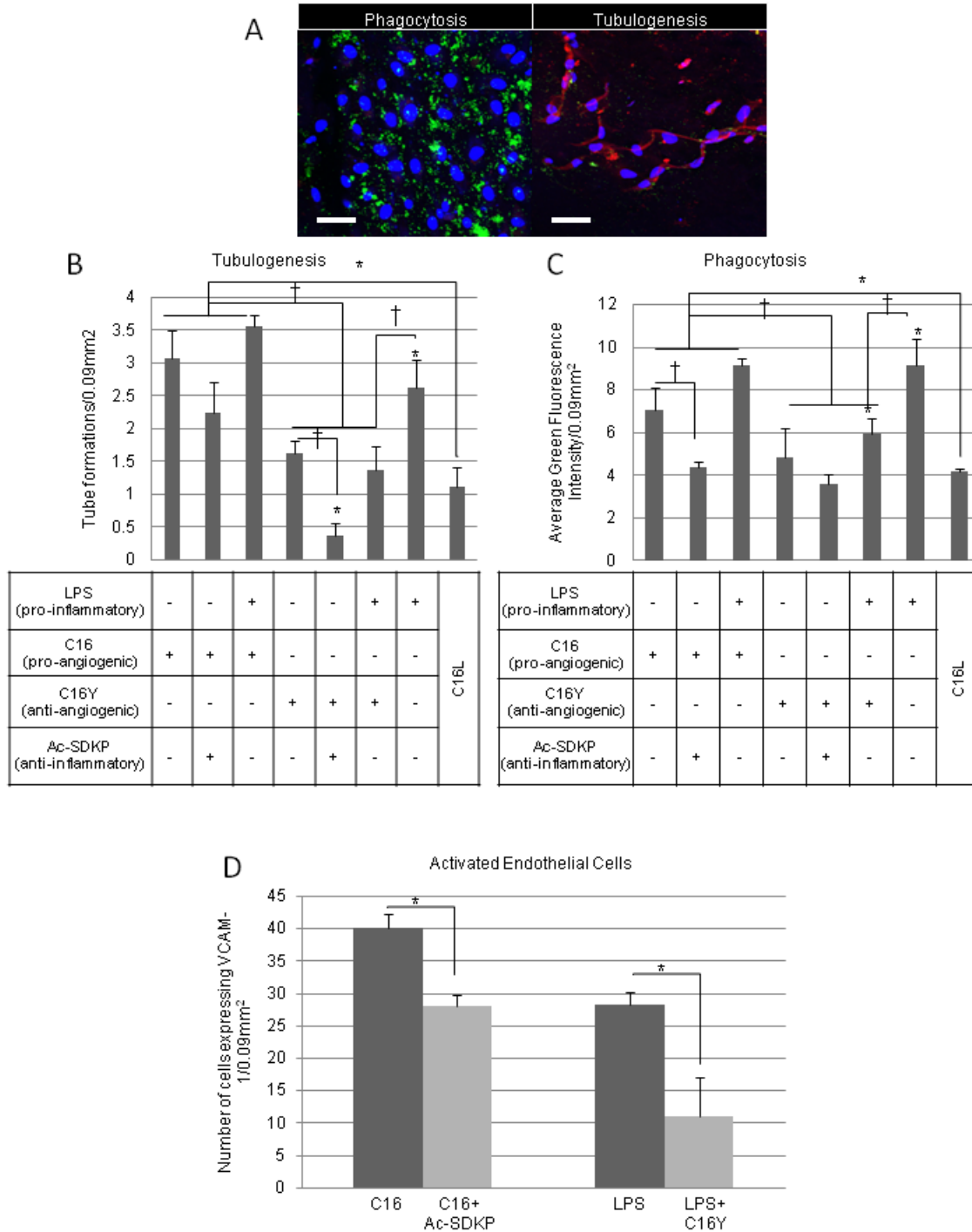


Figure 5. *In vitro* co-culture of macrophages and HUVECs with combinations of peptides in collagen-hydrogel scaffolds. A. Fluorescence images showing activated macrophages phagocytizing *E.coli* particles (green, top left) and HUVECs with VCAM-1 staining (red, top right). Scale bar=50 μ m. **B.** Tubulogenesis of HUVECs. The number of spots showing three or more VCAM-1 positive ECs joined together to form a “tube” was measured in image fields. **C.** Phagocytosis (average green fluorescence per image field) of macrophages. **D.** Inflammatory activation of HUVECs. The number of VCAM-1-positive HUVECs was measured in image fields. **b-d)** n=8. **b-c)** *p<0.05 vs. control (C16L).

In vivo subcutaneous implantation of collagen-hydrogel scaffolds

In order to test the effects of LPS and Ac-SDKP on activation of inflammatory cells, F4/80 expression was measured in collagen-hydrogel scaffolds implanted subcutaneously in mice for seven days. Red fluorescence intensity from immunostaining of F4/80 antigens was measured and normalized to cell number. Treatment with LPS showed the highest level of F4/80 expression while treatment with anti-inflammatory Ac-SDKP showed the lowest level of F4/80 expression (Figure 6a and b). The addition of pro-angiogenic C16 to collagen-hydrogel scaffolds increased the number of F4/80-positive cells, compared to the conditions with anti-inflammatory Ac-SDKP or without peptide treatment.

The formation of new blood vessels (red) and the phagocytosis of inflammatory cells (yellow-green) in implanted collagen-hydrogel scaffolds were also visualized and quantified (Figure 6c). Compared to implants with no peptide, addition of anti-inflammatory Ac-SDKP to collagen-hydrogel scaffolds significantly decreased the number of phagocytosing cells as well as the level of connectivity and branching of vasculature. However, these activities significantly increased when C16 peptides were present in the implants (Figure 6c top). Quantification of vascular perfusion capacity and phagocytosis (Figure 6c top and bottom graphs, respectively) showed similar patterns, in which the implants with Ac-SDKP peptides showed significantly lower levels of the phagocytosis activity and perfusion capacity, compared to the implants with C16 peptides or no treatment. On the other hand, a C16-mediated induction of angiogenesis significantly increased the phagocytosis activity compared to the other test groups. These results showed the two-way communication between inflammatory cells and ECs *in vivo* and show that they regulate each other in response to biomaterial implants.

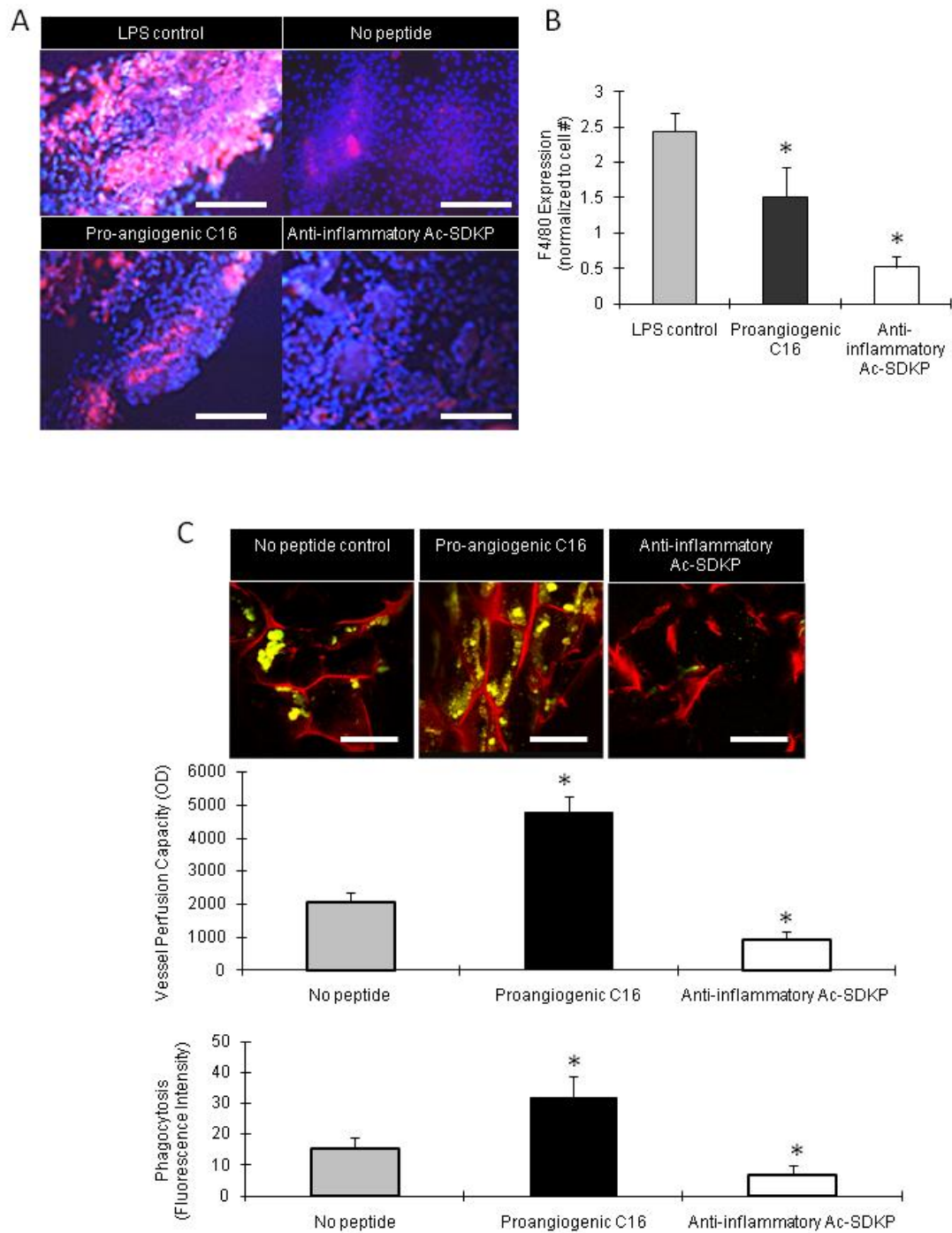


Figure 6. *In vivo* angiogenesis and inflammatory cell activation with peptides in collagen-hydrogel scaffolds. A. Fluorescence images showing F4/80-positive macrophages (red) out of cells (blue nuclei) infiltrated into implanted scaffolds with LPS (100ng) (top left), C16 (75 μ g) (bottom left), Ac-SDKP (75 μ g) (bottom right), or no peptide (top right). **B.** The intensity of red fluorescence (F4/80) was normalized to the corresponding cell number (graph), indicating the degree of macrophage activation. **C.** Fluorescence images showing new blood vessels (red), which were visualized by fluorescent microangiography, and macrophages phagocytosing *E.coli* particles (yellowish green) in scaffold implants with no peptide (top left), C16 (75 μ g) (top middle), or Ac-SDKP (75 μ g) (top right). Scale bar = 100 μ m. b-c) * p < 0.05 vs. a control group (no peptide or LPS).

Discussion

The primary goal of this study was to elucidate a mechanism of communication between angiogenesis and inflammation in biomaterial implants. The results indicate that angiogenesis and inflammation are interconnected through feedback mechanisms. In particular, the causative roles of inflammatory cell activation in angiogenesis are evident by effects of pro-or anti-inflammatory molecules on angiogenic activity. This feedback relationship must be taken into consideration when optimizing the host response to biomaterial implants. This study suggests that the host immune response should be properly preserved and controlled to enhance angiogenesis for functional survival of biomaterial implants.

A series of PEG-cross-linked tyrosine-derived poly (X%DTE-co-Y%DT carbonates) provided a modifiable template for creating porous hydrogel scaffolds through salt leaching and phase separation. These scaffolds proved to be highly porous, with a high degree of interconnectivity that aided oxygen and nutrient transport, cell growth, and migration into internal layers of hydrogel scaffolds. Unlike many common hydrogels, which become stiffer as cross-linking degree increases, these hydrogels become more hydrophilic and compliant with increasing crosslink density most likely due to increased water absorption by PEG-cross-linkers [26, 38]. As the PEG content increased from 0% to 8% and to 20% in the mixture with (90%DTE-co-10%DT carbonate), the thickness of the accumulated fibrin layer significantly decreased, confirming the PEG-mediated repellent effect on protein adsorption [39, 40]. The cross-linking density also influences the degradation rate, which is important for controlling angiogenesis and tissue regeneration. Increasing the cross-linking density decreased the degradation rate of the hydrogel scaffold. This is most likely due to increased covalent bonds formed among polymer chains through cross-linking, which slow the disintegration rate of the hydrogel. These hydrogel scaffolds can serve as a unique system for studying angiogenesis and inflammation by controlling the crosslink density and pore structure, thereby controlling the mechanical properties and degradation rate.

Introduction of synthetic peptides, pro-angiogenic C16, anti-angiogenic C16Y, control peptide C16L, and anti-inflammatory Ac-SDKP, as well as the pro-inflammatory molecule LPS, allowed for the control of inflammation and angiogenesis. These peptides were incorporated into the hydrogel by hybridization with a collagen gel, which proved to remain stable over time, allowing sustained release of the peptides from the collagen-hydrogel scaffolds. The peptides used in this study came from two distinct

groups: long peptides (including C16, C16Y, and C16L) and short peptides (including Ac-SDKP and Ac-DKSP). Both types of peptides were released from the scaffold in a sustained manner over time, but long peptides showed a faster burst release than the short peptides. After 14 days, however, both short and long peptides released almost the same amount. This sustained release allows cells to be exposed to peptides extended periods of time. The pro-angiogenic effect of the C16 peptide was verified by the increase in endothelial cell migration into the scaffold, and the increase in tube formation compared to conditions without C16 peptide. Collagen-filled hydrogel scaffolds with Ac-SDKP reduced phagocytosis, compared to scaffolds without Ac-SDKP or with pro-inflammatory LPS.

When macrophages and ECs were co-cultured in peptide and collagen-filled hydrogel scaffolds, the same trend in both EC tubulogenesis and macrophage phagocytosis was observed in response to variations in the types and combination of functional peptides, indicating interconnectivity between the two cell activities (Figure 5). In the presence of anti-inflammatory Ac-SDKP, both phagocytosis and tubulogenesis decreased while both activities increased in the presence of pro-angiogenic C16. In response to the combination of anti-angiogenic C16Y with anti-inflammatory Ac-SDKP, both phagocytic activity and tubulogenesis were minimized, while both activities were maximized in response to the combination of pro-angiogenic C16 with pro-inflammatory LPS. C16, with or without the addition of pro- or anti-inflammatory molecules, induced higher levels of both tube formation and phagocytic activity than C16Y, with or without the addition of pro- or anti-inflammatory molecules, indicating that although angiogenesis increased upon the addition of pro-inflammatory LPS and decreased upon the addition of Ac-SDKP, these changes cannot fully compensate for the effects of pro-angiogenic C16 and anti-angiogenic C16Y. These results show that the communication between angiogenesis and inflammation is not one-sided. Moreover, the two-way feedback interactions between inflammatory responses and angiogenic processes suggest that elimination of host inflammatory responses through modification of biomaterial properties may impede tissue interactions with implants and further regeneration by impairing blood vessel formation.

In vivo experiments verified the cross-talk between angiogenesis and inflammation in biomaterial implants as collagen-hydrogel scaffolds containing anti-inflammatory Ac-SDKP had fewer activated phagocytic cells, but also revealed fewer functional blood vessels with less branching compared to

scaffolds with no peptide or C16 treatment. Collagen-hydrogel scaffolds containing pro-angiogenic C16 recruited many phagocytic cells, particularly near the newly-formed blood vessels, and therefore showed significantly higher levels of perfusion capacity and phagocytosis activity compared to scaffolds containing Ac-SDKP. The same result was also observed in the immunohistochemistry analysis of excised implants. F4/80 antigen expression, as seen on a wide range of activated inflammatory cells (e.g. mature tissue macrophages) [41], was higher with C16 treatment than with no peptide or Ac-SDKP treatment. These results indicate that inflammatory cell response may contribute to the formation of intact functional blood vessels in the implants *in vivo*, but this response is not one-sided. Inflammatory cells influence ECs and ECs influence inflammatory cells in a bi-directional method of communication.

Emerging evidence points to the probability that inflammatory changes regulate the neovascularization that is associated with wound healing, tumor growth, and inflammatory disease, such as psoriasis, arthritis, and atherosclerosis. Inflammatory cells recruited to the inflamed or injured tissue can release growth factors as well as proteases capable of modulating tissue structure and promoting angiogenesis [5]. Several studies revealed that the degree of inflammation was related to the level of vascularization of the biomaterial implants [9, 10]. The pro-angiogenic vascular endothelial growth factor (VEGF) has potent vascular permeability-enhancing properties in addition to being a chemo-attractant for mononuclear cells. Activated human inflammatory cells, such as peripheral blood mononuclear cells and neutrophils, express VEGF [8, 42], indicating another inflammatory-mediated pathway important in angiogenic activities. In future studies we will investigate the mechanism of this communication and identify how these specific factors play a role in inflammatory cell-mediated angiogenesis. The elucidation of a clear mechanism will provide an efficient and realistic paradigm of the interconnectivity of inflammation with angiogenesis for the functional survival of biomaterial implants. The current study provides a new concept for biomaterial design which utilizes flexible inflammatory parameters to control angiogenesis for the eventual success of therapeutic interventions.

CHAPTER III

CONCLUSION

A clear interconnectivity between angiogenic and inflammatory activities was found from *in vitro* and *in vivo* studies using bioactive hydrogel scaffolds hybridized with functional peptides, indicating an inflammatory mechanism regulating follow-up angiogenic processes in hydrogels. This study suggests that the host immune response should be properly preserved and controlled to enhance angiogenesis for functional survival of biomaterial implants. Elucidating the mechanisms behind the communication of these two processes will provide a method for the optimization of host response to biomaterials.

REFERENCES

- [1] Bailey LO, Washburn NR, Simon CG, Chan ES, Wang FW. Quantification of inflammatory cellular responses using real-time polymerase chain reaction. *J Biomed Mater Res A*. 2004;69A:305-13.
- [2] Hu WJ, Eaton JW, Tang LP. Molecular basis of biomaterial-mediated foreign body reactions. *Blood*. 2001;98:1231-8.
- [3] Lutolf MP, Hubbell JA. Synthetic biomaterials as instructive extracellular microenvironments for morphogenesis in tissue engineering. *Nat Biotechnol*. 2005;23:47-55.
- [4] Bachetti T, Morbidelli L. Endothelial cells in culture: A model for studying vascular functions. *Pharmacol Res*. 2000;42:9-19.
- [5] Shamamian P, Schwartz JD, Pocock BJ, Monea S, Whiting D, Marcus SG, et al. Activation of progelatinase A (MMP-2) by neutrophil elastase, cathepsin G, and proteinase-3: a role for inflammatory cells in tumor invasion and angiogenesis. *J Cell Physiol*. 2001;189:197-206.
- [6] Scapini P, Nesi L, Morini M, Tanghetti E, Belleri M, Noonan D, et al. Generation of biologically active angiostatin kringle 1-3 by activated human neutrophils. *J Immunol*. 2002;168:5798-804.
- [7] Lee S, Zheng M, Kim B, Rouse BT. Role of matrix metalloproteinase-9 in angiogenesis caused by ocular infection with herpes simplex virus. *J Clin Invest*. 2002;110:1105-11.
- [8] Webb NJ, Myers CR, Watson CJ, Bottomley MJ, Brenchley PE. Activated human neutrophils express vascular endothelial growth factor (VEGF). *Cytokine*. 1998;10:254-7.
- [9] Sung HJ, Meredith C, Johnson C, Galis ZS. The effect of scaffold degradation rate on three-dimensional cell growth and angiogenesis. *Biomaterials*. 2004;25:5735-42.
- [10] Sung HJ, Johnson CE, Lessner SM, Magid R, Drury DN, Galis ZS. Matrix metalloproteinase 9 facilitates collagen remodeling and angiogenesis for vascular constructs. *Tissue Eng*. 2005;11:267-76.
- [11] Chung TW, Yang MG, Liu DZ, Chen WP, Pan CI, Wang SS. Enhancing growth human endothelial cells on Arg-Gly-Asp (RGD) embedded poly (epsilon-caprolactone) (PCL) surface with nanometer scale of surface disturbance. *J Biomed Mater Res A*. 2005;72A:213-9.
- [12] Xu CY, Yang F, Wang S, Ramakrishna S. In vitro study of human vascular endothelial cell function on materials with various surface roughness. *J Biomed Mater Res A*. 2004;71A:154-61.
- [13] Zhao X, Harris JM. Novel degradable poly(ethylene glycol) hydrogels for controlled release of protein. *J Pharm Sci*. 1998;87:1450-8.
- [14] Bryant SJ, Anseth KS. Hydrogel properties influence ECM production by chondrocytes photoencapsulated in poly(ethylene glycol) hydrogels. *J Biomed Mater Res*. 2002;59:63-72.
- [15] Pieper JS, van Wachem PB, van Luyn MJA, Brouwer LA, Hafmans T, Veerkamp JH, et al. Attachment of glycosaminoglycans to collagenous matrices modulates the tissue response in rats. *Biomaterials*. 2000;21:1689-99.
- [16] Sieminski AL, Gooch KJ. Biomaterial-microvasculature interactions. *Biomaterials*. 2000;21:2233-41.
- [17] Dziubla TD, Lowman AM. Vascularization of PEG-grafted macroporous hydrogel sponges: A three-dimensional in vitro angiogenesis model using human microvascular endothelial cells. *J Biomed Mater Res A*. 2004;68A:603-14.
- [18] Yu C, Kohn J. Tyrosine-PEG-derived poly(ether carbonate)s as new biomaterials. Part I: synthesis and evaluation. *Biomaterials*. 1999;20:253-64.
- [19] Burkoth AK, Burdick J, Anseth KS. Surface and bulk modifications to photocrosslinked polyanhydrides to control degradation behavior. *J Biomed Mater Res*. 2000;51:352-9.
- [20] Ponce ML, Hibino S, Lebioda AM, Mochizuki M, Nomizu M, Kleinman HK. Identification of a potent peptide antagonist to an active laminin-1 sequence that blocks angiogenesis and tumor growth. *Cancer Res*. 2003;63:5060-4.

- [21] Malinda KM, Nomizu M, Chung M, Delgado M, Kuratomi Y, Yamada Y, et al. Identification of laminin alpha1 and beta1 chain peptides active for endothelial cell adhesion, tube formation, and aortic sprouting. *FASEB J.* 1999;13:53-62.
- [22] Yang F, Yang XP, Liu YH, Xu J, Cingolani O, Rhaleb NE, et al. Ac-SDKP reverses inflammation and fibrosis in rats with heart failure after myocardial infarction. *Hypertension.* 2004;43:229-36.
- [23] Cavin MA. Therapeutic potential of thymosin-beta4 and its derivative N-acetyl-seryl-aspartyl-lysyl-proline (Ac-SDKP) in cardiac healing after infarction. *Am J Cardiovasc Drugs.* 2006;6:305-11.
- [24] Cingolani OH, Yang XP, Liu YH, Villanueva M, Rhaleb NE, Carretero OA. Reduction of cardiac fibrosis decreases systolic performance without affecting diastolic function in hypertensive rats. *Hypertension.* 2004;43:1067-73.
- [25] Rasoul S, Carretero OA, Peng HM, Cavin MA, Zhuo JL, Sanchez-Mendoza A, et al. Antifibrotic effect of Ac-SDKP and angiotensin-converting enzyme inhibition in hypertension. *J Hypertens.* 2004;22:593-603.
- [26] Sung HJ, Labazzo KMS, Bolikal D, Weiner MJ, Zimnisky R, Kohn J. Angiogenic competency of biodegradable hydrogels fabricated from polyethylene glycol-crosslinked tyrosine-derived polycarbonates. *Eur Cells Mater.* 2008;15:77-86.
- [27] Kuratomi Y, Nomizu M, Tanaka K, Ponce ML, Komiyama S, Kleinman HK, et al. Laminin gamma 1 chain peptide, C-16 (KAFDITYVRLKF), promotes migration, MMP-9 secretion, and pulmonary metastasis of B16-F10 mouse melanoma cells. *Br J Cancer.* 2002;86:1169-73.
- [28] Wan Y, Yu A, Wu H, Wang Z, Wen D. Porous-conductive chitosan scaffolds for tissue engineering II. in vitro and in vivo degradation. *J Mater Sci Mater Med.* 2005;16:1017-28.
- [29] Sung HJ, Luk A, Murthy NS, Liu E, Jois M, Joy A, et al. Poly(ethylene glycol) as a sensitive regulator of cell survival fate on polymeric biomaterials: the interplay of cell adhesion and pro-oxidant signaling mechanisms. *Soft Matter.* 2010;6:5196-205.
- [30] Voinova MV, Rodahl M, Jonson M, Kasemo B. Viscoelastic acoustic response of layered polymer films at fluid-solid interfaces: Continuum mechanics approach. *Phys Scripta.* 1999;59:391-6.
- [31] Weber N, Pesnell A, Bolikal D, Zeltinger J, Kohn J. Viscoelastic properties of fibrinogen adsorbed to the surface of biomaterials used in blood-contacting medical devices. *Langmuir.* 2007;23:3298-304.
- [32] Sung HJ, Yee A, Eskin SG, McIntire LV. Cyclic strain and motion control produce opposite oxidative responses in two human endothelial cell types. *Am J Physiol-Cell Ph.* 2007;293:C87-C94.
- [33] Nau GJ, Richmond JF, Schlesinger A, Jennings EG, Lander ES, Young RA. Human macrophage activation programs induced by bacterial pathogens. *Proc Natl Acad Sci U S A.* 2002;99:1503-8.
- [34] Foukas LC, Katsoulas HL, Paraskevopoulou N, Metheniti A, Lambropoulou M, Marmaras VJ. Phagocytosis of *Escherichia coli* by insect hemocytes requires both activation of the Ras/mitogen-activated protein kinase signal transduction pathway for attachment and beta3 integrin for internalization. *J Biol Chem.* 1998;273:14813-8.
- [35] Wan CP, Park CS, Lau BH. A rapid and simple microfluorometric phagocytosis assay. *J Immunol Methods.* 1993;162:1-7.
- [36] Johnson C, Sung HJ, Lessner SM, Fini ME, Galis ZS. Matrix metalloproteinase-9 is required for adequate angiogenic revascularization of ischemic tissues - Potential role in capillary branching. *Circ Res.* 2004;94:262-8.
- [37] Xue. PU/PTFE-stimulated monocyte-derived soluble factors induced inflammatory activation in endothelial cells. *Toxicology in Vitro.* 2010:404-10.
- [38] Sun G, Zhang XZ, Chu CC. Effect of the molecular weight of polyethylene glycol (PEG) on the properties of chitosan-PEG-poly(N-isopropylacrylamide) hydrogels. *J Mater Sci Mater Med.* 2008;19:2865-72.

- [39] Mori Y, Nagaoka S, Takiuchi H, Kikuchi T, Noguchi N, Tanzawa H, et al. A new antithrombogenic material with long polyethyleneoxide chains. *Trans Am Soc Artif Intern Organs*. 1982;28:459-63.
- [40] Tziampazis E, Kohn J, Moghe PV. PEG-variant biomaterials as selectively adhesive protein templates: model surfaces for controlled cell adhesion and migration. *Biomaterials*. 2000;21:511-20.
- [41] Brem-Exner BG, Sattler C, Hutchinson JA, Koehl GE, Kronenberg K, Farkas S, et al. Macrophages driven to a novel state of activation have anti-inflammatory properties in mice. *J Immunol*. 2008;180:335-49.
- [42] Griga T, Gutzeit A, Sommerkamp C, May B. Increased production of vascular endothelial growth factor by peripheral blood mononuclear cells in patients with inflammatory bowel disease. *Eur J Gastroenterol Hepatol*. 1999;11:175-9.